Available online at www.sciencedirect.com
SCIENCE DIRECT®
Journal of Nuclear Materials 337–339 (2005) 251–255
journal of nuclear materials
www.elsevier.com/locate/jnucmat

Accounting of the power balance for neutral-beam heated H-mode plasmas in NSTX

S.F. Paul [a,*], R. Maingi [b], V. Soukhanovskii [c], S.M. Kaye [a], H.W. Kugel [a], The NSTX Research Team

[a] *Princeton Plasma Physics Laboratory, U.S. Route #1, North, Princeton, NJ 08543-0451, USA*
[b] *Oak Ridge National Laboratory, Oak Ridge, TN, USA*
[c] *Lawrence Livermore National Laboratory, Livermore, CA, USA*

Abstract

Power balance accountability was investigated for neutral beam heated plasmas in NSTX. Measurements of heat to the divertor strike plates and radiation in the divertor and the core were made as a function of heating power in lower single-null (LSN) and double-null (DN) configurations. Up to 70% of the net input power is accounted in the LSN discharges with ≈15–20% of power lost as fast ions, ≈25–35% incident on the divertor plates, ≈5% radiated in the core, and ≈5–10% radiated in the divertor. In DN discharges, the fast ion loss is comparable to LSN discharges, the core radiated power fraction is ≈10%, and the power deposited in the lower divertor as radiation and heat flux is ≈20–25% of the total. Assuming up/down symmetry, the power accountability in DN is ≈85–90%.

PACS: 52.40.H; 52.55.Fa
Keywords: Divertor; Edge plasma; Power balance; NSTX

1. Introduction

Accounting of power balance is needed for the understanding of divertor operation, a requirement for future high-power fusion devices. This paper presents results from a power accountability experiment on the National Spherical Torus Experiment (NSTX) [1] whose small major radius (intrinsic to spherical tokamak designs) can lead to high heat fluxes to plasma facing components (PFC's). For this experiment, NSTX (R = 0.85 m, a = 0.67 m, $R/a \geqslant 1.26$) was operated at I_p = 0.8 MA, B_t = 0.45 T in lower single-null (LSN) and double-null diverted (DN) configurations over a range of neutral beam injected (NBI) power from 1 to 6 MW. H-modes, which have confinement properties desirable in high power, long-pulse reactors, are routinely produced in diverted discharges in NSTX. Shown in Fig. 1 are the typical conditions of the LSN H-mode discharges, which generally exhibit occasional large type I ELMs at ~20 Hz. accompanied by newly observed, small amplitude ELMs, recently termed 'type V' [2].

Previous results from NSTX [3] showed that the heat flux to the divertor plates in LSN H-modes reached 10 MW/m^2 with 4.9 MW of NBI power, accounting for between 50% and 70% of the SOL power. Here we

* Corresponding author. Tel.: +1 609 243 3781; fax: +1 609 243 2418.
E-mail address: spaul@pppl.gov (S.F. Paul).

0022-3115/$ - see front matter
doi:10.1016/j.jnucmat.2004.10.153

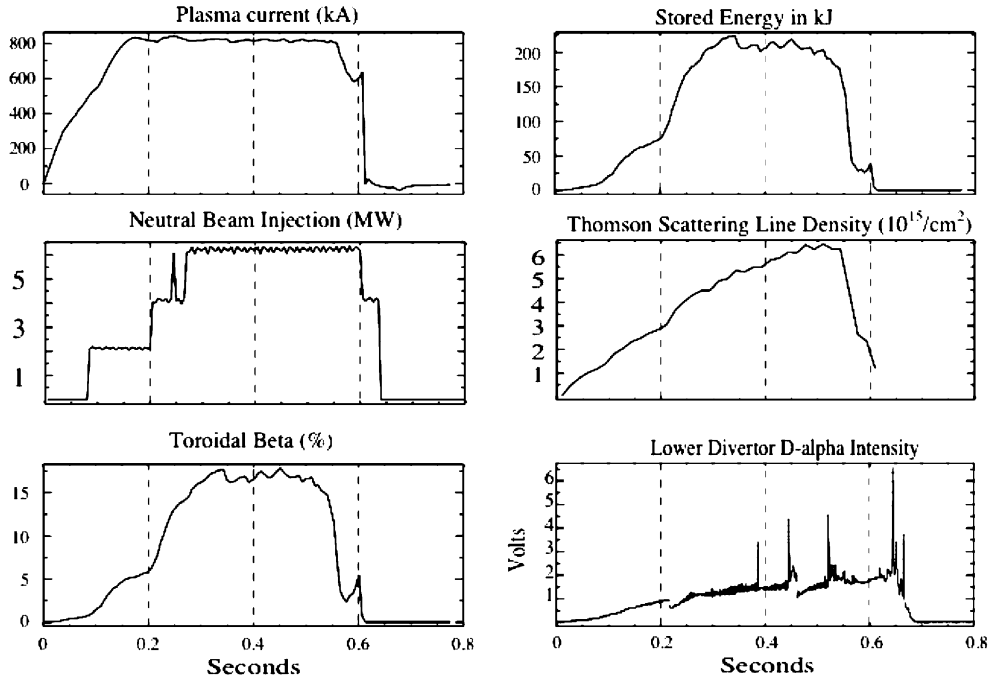

Fig. 1. Operating conditions for the LSN power scan in H-modes. The plasma current is in amperes, the Injected power is in megawatt, and the D_α signal is in arbitrary units. This plasma (shot #112499) had a nominal NBI power of 6 MW and a plasma current of 0.8 MA. The H-mode transition occurred at 0.22 s and the first type I ELM occurred at 0.34 s.

augment that study with a fine NBI power scan and more detailed radiated power measurements. The power scan was achieved by changing the number of neutral beam sources (each providing 2.0 MW at 90 kV), while keeping NBI voltage, plasma current and shape constant and holding the central electron density in the $4.0–4.7 \times 10^{13}$ cm^{-3} range. To allow for thermal equilibration, discharges were designed to remain in H-mode for a minimum of 100 ms.

The power flow regime (i.e. sheath limited, conduction recycling, or detached) in the divertor plasma is known to affect the balance between the inner and outer target power flow, as well as the balance between radiated power and heat flux [4]. The divertor D_α and D_γ profiles from 1-D CCD cameras, along with the ion saturation current measured by the lower divertor tile Langmuir probes, indicate that the NSTX inner divertor is detached and the outer divertor is attached in nearly all of the conditions presented here [5].

Power balance studies from the conventional aspect ratio ($R/a \geqslant 2.7$) DIII-D tokamak [6] and also the low aspect ratio ($R/a \geqslant 1.3$) MAST device have been performed [7]. In LSN H-mode discharges on DIII-D, the total power accountability was more than 85%, with a core radiated power fraction $\leqslant$18%, and an inner/outer divertor power split of 1/1.3 [6]. In the MAST device [7], the in/out power split in DN discharges was quite high (1:9), but qualitatively consistent with NSTX and other devices operating in DN configurations. That study utilized Langmuir probes in the target; no accounting of radiated power was given.

2. Diagnostics – bolometric and infrared camera measurements

Employing AXUV photodiodes, the core radiated power density (emissivity) at the plasma midplane is determined through Abel-inversion of the data from a 16-channel bolometer array that views tangentially across the midplane of the entire plasma column. The dominant uncertainty in the *total* radiated power results from the assumption necessary to extrapolate the midplane data over the entire plasma volume. The midplane data are projected along poloidal flux contours, obtained from EFIT equilibrium reconstructions, assuming that the radiated power is a constant along a surface of constant $-\psi$. Because the midplane emissivity profile is asymmetric about the magnetic axis with in/out ratios for the same ψ-surface as high as 10:1, the total radiated power is calculated by using a power density that is the average of the inner and outer values on the same ψ surface. This result-

ing uncertainty in the core radiation measurement is up to ±50% depending on whether the inboard or outboard profile values are used instead of the average.

A second concern about the core radiated power measurement is that the AXUV photodiodes have a known reduction in sensitivity to photons with energy <30 eV [8]. This is an important consideration because the Abel-inverted profiles are peaked at the edge in these (and most) NSTX discharges, as confirmed independently with Ultra-Soft X-ray spectroscopy and visible continuum measurements. In addition, charge-exchange spectroscopy shows high edge carbon emission and that the CIII, CIV, and CVI visible radiation is emitted within 2–3 cm of the separatrix. The published response curves for the relevant edge carbon lines, principally 154.8 nm (8.0 eV, CIV) and 97.7 nm (12.7 eV, CIII) are used to compensate for the variation in the detector's sensitivity. The response to photons in the 8–12 eV range is, on average, 2.6 times less sensitive than photons with >50 eV. Therefore after the Abel inversion, the emissivities in the outer 3 cm inside the separatrix are multiplied by 2.6. This adjustment has the effect of increasing the total radiated power by about 15%. The adjustment would increase to 25% if applied within 7 cm of the separatrix, corresponding to the spatial resolution of each bolometer channel.

Recently a 'JET style' [9] 4-channel divertor bolometer array was installed, consisting of a 4 μm gold foil on a 20 μm mica substrate that is able to tolerate repeated baking cycles up to 160 °C. The foil is also sensitive to charge exchange losses in the divertor chamber. Systematic errors in measuring the heat flux incident on the detectors are less than 10%. To obtain the total radiated power in the divertor, the bolometer channels that view radially inward through the *X*-point to the lower divertor plate are integrated vertically and the toroidal integration is performed by assuming toroidal symmetry. The dominant uncertainty is in the major radius of the radiating volume (needed for the toriodal integration), which is not measured because the divertor bolometer has only horizontally viewing channels. The uncertainty in the divertor radiated power, determined by the uncertainty in the radial distribution of the radiation (between the inner strike point at 0.25 m and the outer strike point at 0.77 m) is −55%, +40%.

An infrared (IR) camera was used to make measurements of divertor heat flux. The camera is a microbolometer array sensitive in the 7–13 μm wavelength range, with a 30 Hz frame rate and a 25 ms thermal e-folding time [10]. Though this heat flux analysis works well for tokamak PFCs in a net erosion area (e.g. the attached outer divertor leg), it can overestimate the heat flux to areas with thin surface coatings and possibly poor thermal contact with the underlying graphite (e.g. the detached inner divertor leg) [11]. The estimated error resulting from the analysis technique is ±20%.

3. Results

In this section, we discuss the power measured by the diagnostics described in the previous section. For reference, the input power is defined as $P_{in} = P_{NBI} + P_{OH} - dW/dt$, where P_{OH} = ohmic power (approximately plasma current times loop voltage) and dW/dt = time derivative of stored energy in both the plasma and the poloidal magnetic field. These values are calculated using the EFIT equilibrium reconstruction code [12,13]. Ignoring the error in dW/dt because most of these discharges are in equilibrium, the uncertainty in P_{in} is dominated by the ±15% error in the calibration of the NBI calorimeters, followed by a 5–7% error in the calculation of P_{OH}.

As shown in Fig. 2, the AXUV diode data show that the radiation from the main plasma is quite low, never exceeding 350 kW and accounting for 2–14% of P_{in}, considerably lower than in DIII-D. As mentioned in Section 2, the edge emission profiles are quite narrow and localized within 2–3 cm of the plasma edge, resulting in a small radiating volume and a low total radiated power. Perhaps more surprising is the fact that the total radiated power decreases by almost a factor of 3 with increasing P_{in}. This can be seen in Fig. 2 with the clear exception of the points where $P_{in} \approx 1$ MW. These two discharges are distinguished from the remainder in that at the time of interest (from .3 to .34 s) dW/dt changes substantially, accounting for about 60% of P_{in}. For the remainder of the points, dW/dt is only a few percent of P_{in}. The principal trend towards decreasing radiated power in the main plasma with increasing P_{in} cannot be explained solely by density changes, either on average or in the edge region where the carbon is radiating. Thomson scattering density profiles show that the line-averaged density varied in a narrow range: from 4 to 4.5×10^{13} cm^{-3} and the edge density only between 1.7 and 2×10^{13} cm^{-3}.

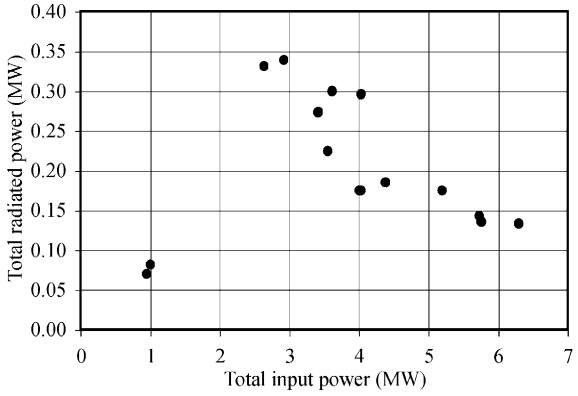

Fig. 2. Total radiated power from the main plasma as a function of input power.

The largest fraction of P_{in} flows to the inboard and outboard divertors. Specifically 25–30% of P_{in} flows to the targets with the in/out split typically 1:4 in LSN plasmas. The peak heat flux to the outer divertor strike plates increases with NBI power up to 7 MW/m^2 at 6 MW and is typically 3–6 times the peak heat flux to the inner divertor. The exception is the low input power shots, where this ratio is about 1:15. In DN discharges from this experiment, the power split is approximately 1:9, similar to the MAST results mentioned previously. The peak line-averaged emissivity measured by the divertor bolometer channel also increases linearly with P_{in} but at a level of about 5% of the peak heat flux to the outer divertor plate. With the radial location of the emitting volume assumed to be midway between the X-point and the outer strike point, the volume-integrated power radiated in the divertor accounts for between 10% and 15% of P_{in}.

Finally, fast ion losses were calculated using the TRANSP code, and show that a significant fraction (10–20%) of P_{in} is lost due to three processes. Bad orbit losses, NBI shine-through, and prompt charge-exchange account for 50%, 40%, and 10% of the fast ion losses, respectively. The expected uncertainty in the fast-ion loss calculations is about 30%. The lost ions are predicted to strike surfaces not observed by the IR cameras in NSTX.

A composite plot of the power measurements and calculations discussed above is shown in Fig. 3 as a function of P_{in}. To summarize: the LSN operation results show that 70% of P_{in} is accounted for. The mean values and uncertainties in the individual power loss channels are: 18 ± 6% of power lost as fast ions – prompt CX, bad orbits, and shine through, 31 ± 6% incident on the divertor plates, 14 ± 7% radiated in the divertor, and 7 ± 4% radiated in the main plasma. The sum of the squares of the estimated uncertainties in the individual measurements and calculations is about 10% of P_{in}. This is smaller than the observed 22% standard deviation in the total power accountability for the thirteen discharges in the LSN power scan, however, the variability is dominated by the 0.7 MW shot that over accounts for the input power (see Fig. 3). Discounting that shot due to the high dW/dt, the variability in the data is only 5.5%, so investigating the cause of the unexpectedly high variability is probably not warranted.

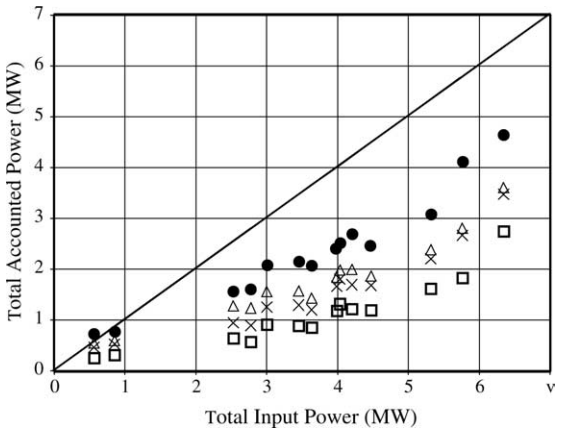

Fig. 3. Incremental contributions to the total accounted power for the H-mode power scan in LSN. The open squares (□) depict the heat flow to the divertor plates. The increment between the □'s and the ×'s represent the divertor radiation. The increment between the ×'s and the triangles (△) is due to radiation from the main plasma. The energy expended in orbit losses is shown by the increment between the △'s and the ●'s. The ●'s represent the total accounted power.

4. Discussion

We consider possible diagnostic issues that may lead to an underestimate of the power lost through various channels. First, we compensated for the decreased sensitivity of the AXUV diodes to low-energy photons within 3 cm of the edge. Applying the sensitivity correction deeper in the plasma would imply significant radiation from low-charge state carbon in the edge pedestal and hotter core regions, which is not supported by other measurements. Second, the uncertainty in the location of the radiation zone viewed by the divertor bolometers would lead to an underestimate of the divertor radiation only if it originated mainly from the outer strike point region. However the detachment studies and divertor imaging with fast cameras has shown that the radiation is more likely further *inboard* than our assumption, i.e. the divertor radiation is likely to be over-estimated. Third, the issues discussed regarding the interpretation of the IR camera data indicate that the heat flux might be overestimated in the presence of surface layers, but not under-estimated.

There is the possibility that the missing power could be due to thermal charge exchange losses. The main chamber bolometers are insensitive to neutrals, but TRANSP calculations indicate that the thermal charge exchange losses account for less than 5% of P_{in}. In DIII-D, the charge exchange losses typically peak in the X-point region, an area not surveyed by the core bolometry in NSTX. However the divertor bolometers are sensitive to charge exchange and do sample the X-point region. Moreover a significant portion of charge exchange losses are expected to heat the target plates in the private flux region between the strike point, an area observed by the IR camera. Hence we conclude that charge exchange losses probably do not account for a large fraction of the missing input power.

Finally there may be power flow to surfaces not measured by the IR camera, namely the center stack, the

outer wall, and top divertor. Preliminary analysis of a new center stack IR camera suggests that little of the power is present there. However, a number of observations suggest that a large fraction of the missing power could be flowing to the upper divertor. Firstly, we inferred significantly better total power accountability (~85% with the assumption of up/down symmetry) in DN discharges with engineering parameters similar to these LSN discharges. Secondly, in DN discharges, 20–25% of P_{in} flowed to the lower divertor. Assuming up/down symmetry, the power to the single divertor in a fully LSN plasma configuration should be *twice* that in the corresponding symmetric DN plasma, e.g. 40–50% of P_{in}, yet only 25–35% flowed to the lower divertor in comparable LSN plasmas. Thirdly, the LSN shape used in this experiment had a second separatrix about 1.2 cm beyond the first separatrix (projected to the outer midplane) as characterized by EFIT's *drsep* parameter. In comparison, the divertor heat flux width was 3–6 cm. This divertor width can be mapped upstream using the EFIT-computed poloidal flux expansion factor of 5 from the outer midplane to the lower divertor, giving a midplane power flux width between 0.6 and 1.2 cm. Given the uncertainties in the EFIT magnetic mapping, we conclude that the midplane SOL power flux width was ~*drsep*, and as a consequence as much as $1/e \sim 40\%$ of the total SOL loss power could flow beyond the first power flux width. Assuming up/down symmetry for the power flow outside the flux width, up to half of that amount (~20%) of the SOL loss power could flow to the upper divertor, with the remaining ~80% flowing to the lower divertor. We also note the sensitivity of power flow to the location of the second separatrix because in previous LSN discharges [3] with a *drsep* value near 2 cm, 60–70% of the SOL power flowed into the lower divertor, a figure close to our estimate. Therefore the equivalent of 1/4 of the lower divertor power flows to the upper divertor. With the lower divertor power accounting for $45 \pm 14\%$ of P_{in}, the upper divertor power is $11 \pm 4\%$ of P_{in}. Incorporating the error in P_{in}, the total accounted power is $81 \pm 16\%$. The hypothesis of power flow to the top divertor will be tested in upcoming experiments with the implementation of an additional IR camera to view the top divertor.

Acknowledgments

Work supported by US Department of Energy contracts DE-AC02-76CH03073, DE-AC05-00OR22725 and W-7405-ENG-36. The authors gratefully acknowledge the contributions of the NSTX technical staff.

References

[1] M. Ono et al., Nucl. Fusion 40 (2000) 557.
[2] R. Maingi, S.A. Sabbagh, C.E. Bush, et al., these Proceedings, doi:10.1016/j.jnucmat.2004.08.023.
[3] R. Maingi, M.G. Bell, R.E. Bell, et al., Nucl. Fusion 43 (2003) 96.
[4] B. LaBombard, J. Goetz, C. Kurz, et al., Phys. Plasmas 2 (1995) 2242.
[5] V.A. Soukhanovskii, R. Maingi, C. Bush, et al., these Proceedings, doi:10.1016/j.jnucmat.2004.10.135.
[6] A.W. Leonard, C.J. Lasnier, J.W. Cuthbertson, et al., J. Nucl. Mater. 325 (1995) 220.
[7] J.-W. Ahn et al., J. Nucl. Mater. 820 (2001) 290.
[8] R.L. Boivin, J.A. Goetz, E.S. Marmar, et al., Rev. Sci. Instrum. 70 (1999) 260.
[9] K.F. Mast, H. Krause, Rev. Sci. Instrum. 56 (1985) 969.
[10] D. Mastrovito, R. Maingi, H.W. Kugel, et al., Rev. Sci. Instrum. 74 (2003) 5090.
[11] C.H. Skinner et al., Phys. Scr. T 103 (2003) 34.
[12] L.L. Lao et al., Nucl. Fusion 25 (1985) 1611.
[13] S.A. Sabbagh et al., Nucl. Fusion 41 (2001) 1601.